Advanced Journal of Chemistry, Section A, 2025, 8(12), 1890-1903

Advanced Journal of Chemistry, Section A

journal homepage: www.ajchem-a.com

Original Research Article

Synthesis, Chemical Characterization and Biological Activity Evaluation of Lamb Meat-Derived Nanocomposite

Reem Suhail Najm[1]*, Agharid A. AL-Rasheed[2], Ammar S. Mohammed[3], Bashiru Garba[4], Mohammed Jwher Saleh[5]

[1]*Department of Physiology, Pharmacology, and Biochemistry, College of Veterinary Medicine, University of Tikrit, Tikrit, Iraq*
[2]*Department of Microbiology, College of Veterinary Medicine, University of Tikrit, Tikrit, Iraq*
[3]*Department of Chemistry, College of Science, University of Kirkuk, Kirkuk, Iraq*
[4] *Department of Public Health, Faculty of Medicine and Health Sciences, SIMAD University, Mogadishu, Somalia*
[5] *Ministry of Education, Salah al-Din Education Directorate, Tikrit, Iraq*

ARTICLEINFO

Article history

Submitted: 2025-05-17
Revised: 2025-06-27
Accepted: 2025-07-13
ID: AJCA-2505-1849
DOI: **10.48309/AJCA.2025.524268.1849**

KEYWORDS

Animal meat
Nanocomposites
Graphite nano sheet
rGo
Antibacterial

ABSTRACT

The synthesis of nano-derivatives from natural sources, provided that nano-graphite is fully synthesized, has received considerable attention. This work utilizes the modified Hummers method and flame carbonization to create and analyze nano-graphite (rG1) and nano-graphene oxide (rGO2) from lamb meat. Infrared spectroscopy (FT-IR), X-ray diffraction (XRD), electron microscopy (FESEM), atomic force microscopy (AFM), thermal gravimetric analysis (TGA, DTG, DSC, NETZCH SAT409PG\PC), and other physical and spectral analysis methods were used to characterize and analyze these compounds. The agar well diffusion technique evaluated the antibacterial activity against *Escherichia coli* and *Staphylococcus aureus*. The results demonstrate that Nano-Graphene Oxide (rGO2) demonstrated significant antibacterial activity against *S. aureus* at doses of 50, 100, and 150 µg/mL, producing inhibition zones of 10 mm, 15.3 mm, and 17.4 mm, respectively. The results demonstrated that nano-graphite (rG1) exhibited no antibacterial activity. This study introduces a novel, accessible, and sustainable approach of synthesizing carbon-based nanoparticles from biological materials for innovative nanotechnology applications.

GRAPHICALABSTRACT

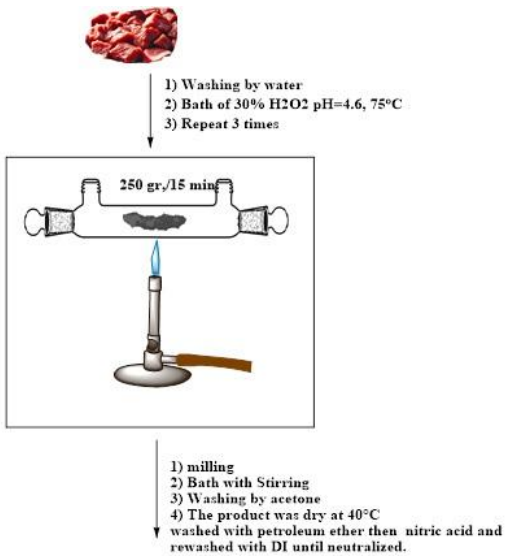

* Corresponding author: Najm, Reem Suhail
✉ E-mail: reemshuil84@tu.edu.iq

Introduction

Integrating chemistry and nanotechnology, nanochemistry is a branch of research that focuses on generating small materials with unique features such as size, shape, interface structure, and defects [1]. In this branch of science, refining is an essential method that employs destructive processes such as distillation or pyrolysis to transform organic material into graphite or substances containing graphite. This occurs when carbon traces remain behind as organic matter breaks down. A minuscule layer of graphite can be, on occasion, removed while preserving the original material's form [2]. Researchers are continually exploring green, reasonable, and accessible methods of creating novel materials in response to growing concerns about the environment, energy problems, and the rising demand for environmentally friendly resources [3]. Due to its reasonable price and sustainability, biomass, a natural and renewable carbon source, has garnered considerable attention [4]. Food scraps, crop residues, and industrial garbage are common biomass waste materials that offer a sustainable means for creating beneficial nanomaterials [5,6]. Due to their unique properties, nanomaterials made up of carbon have generated the most curiosity among them [7,8]. They could come into use in fuel cells for the storage of gases, absorption, catalysis, capture of carbon, the electrodes, cosmetics, and even in cell biology [9,10]. Carbon-rich substances have been efficiently manufactured from some natural sources such as wood charcoal, grain husks, grass, coffee grounds, and leaves from plants. These give a reasonable substitute for expensive graphene-based methods [11]. Carbon-based nanomaterials are created using a variety of techniques, including carbonization, laser ablation, and pyrolysis. The materials produced by each technique vary in size, shape, and structure [12]. Improved nanotechnology is leading to the study and development of more complex graphite-based materials, such as graphene (the natural component that contains carbon nanotubes) and nongraphite dots [13]. The high surface area, outstanding electrical conductivity, strength, and biological compatibility of these materials make them important for a wide range of industrial applications [14,15]. These state-of-the-art nanomaterials are the result of persistently innovative fabrication methods, an abundance of naturally occurring graphite resources, and scalable production processes [16]. This study utilizes lamb meat as a source to synthesize nano-graphite (rG1) and nano-graphene oxide (rGO2), characterize the resulting nanomaterials, and evaluate their antibacterial activity against *E. coli* and *S. aureus*, two pathogenic bacterial strains.

Materials and Methods

Materials

Various substances were utilized in the research: Distilled water, hydrochloric acid (37% of the total), sulfuric acid, nitric acid, ionized water, acetone, petrol ether, permanganate of potassium, nitrate of sodium, nutrient agar media, and Muller Hinton agar media. Each analytical grade with anti-bacterial activity reagents was procured from Scharlau, Poison, and Hi-media.

Synthesis of nano-graphite from lamb meat (rG1)

Lignin removal process

Fresh lamb meat was cut into small pieces, washed thoroughly with distilled water, and immersed in 30% hydrogen peroxide (H_2O_2) at pH 4.6. The solution was heated to 75 °C, and the washing process with hydrogen peroxide was repeated three times. The samples were then rinsed with deionized water three times to

ensure complete removal of residual chemicals [17].

Flame carbonization process

A 250 g sample of pretreated lamb meat was subjected to direct blue flame combustion, and the charred residue was collected within 15 minutes. The collected material was finely ground and washed with 50 mL of acetone, followed by magnetic stirring for 15 minutes. The solution was filtered and dried at 40 °C under atmospheric air and preservation conditions. Subsequently, the dried product was washed with petroleum ether using a water bath at 60-80 °C for 15 minutes. Under regulated conditions, the resulting material underwent filtering and drying. To eliminate contaminants and bring the pH level to 7, the purification process continued with three washes of 10% nitric acid (2 × 45 mL), followed by five deionized water (5 × 45 mL). Two grams of the synthetic material was mixed with five hundred milliliters of deionized water to activate nano-graphite (rG1) for further processing. Afterwards, the suspension was left to leach and fragment by being exposed to ultrasonic irradiation at 50 Hz for 60 minutes. The surface characteristics of the material are improved, making it more reactive, by this technique. Instantaneous centrifugation collection and regulated storage of the activated Nano-Graphite (rG1) followed the ultrasonic treatment.

The modified hummers method for the synthesis of nano-graphene oxide (rGO2)

A modified version of the Hummers method was used to synthesize nano-graphene oxide (rGO2). To begin with, an ice bath was used to distribute the temperature evenly before 46 mL of concentrated sulfuric acid (H_2SO_4) was added. 1.5 g of sodium nitrate ($NaNO_3$) was added to avoid any potential localized overheating while stirring constantly at 0 °C. One gram of nano-graphite (rG1) was gradually added over ten minutes after the acid mixture stabilized, ensuring it was evenly distributed throughout the solution. Afterward, 6 g of potassium permanganate ($KMnO_2$) was cautiously added in 15-minute increments while monitoring the reaction temperature constantly to keep it less than 20 °C. To make sure the combination was completely oxidized; it was swirled magnetically at room temperature for two hours after being withdrawn from the ice bath, which took an extra five minutes. 46 mL of D.W. were added slowly over 20 minutes with constant stirring to start the hydrolysis process. To improve the effectiveness of oxidation, the temperature of the reaction was raised to 98 °C and kept for 20 minutes. In the next phase, 140 mL of distilled water that had been heated to 50 °C was added, and the mixture was left to stir for another 10 minutes at ambient temperature. A 30-minutes stirring period resulted in the production of an olive-green suspension, which signifies effective oxidation, after which 15 mL of 30% hydrogen peroxide (H_2O_2) was added to neutralize any surplus oxidizing agents. And finally, 300 mL of D.W. was added and then the mixture was ept for 24 hours to let it precipitate completely. The oxidized product was efficiently separated by centrifugation at 6000 rpm, and the resulting nano-graphene oxide (rGO2) was recovered. To remove eliminate any remaining metal ions, the material was washed once with 10% hydrochloric acid (HCl). Then, it was washed five times with deionized water (5 × 45 mL) until the solution's pH was neutralized to 7. We ensured the removal of any leftover moisture by drying the purified nano-graphene oxide (GO2) at 60-70 °C until its weight stabilized. This was done before further characterization and utilization [18].

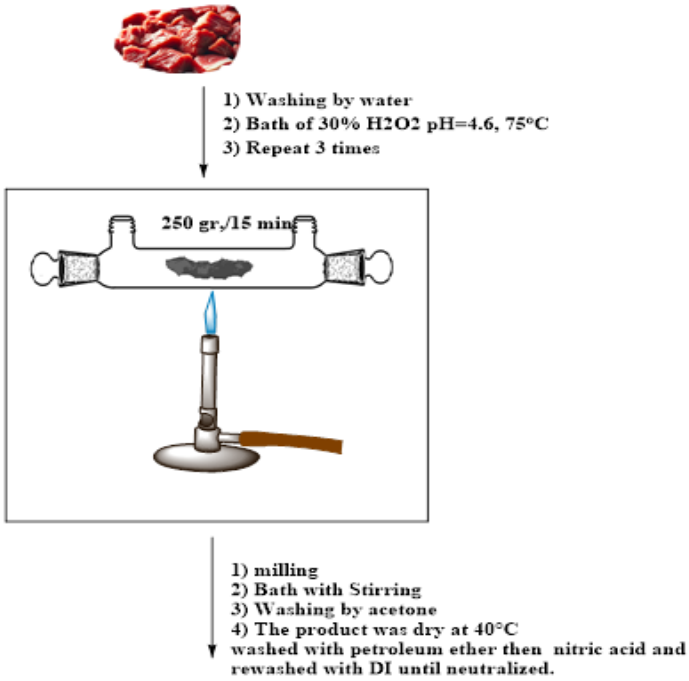

Scheme 1. Synthesis steps of prepared compounds (rG1-rGO2) (chemDrawprofession).

Biological activity for rG1 and rGO2

The agar well diffusion method assessed the bactericidal properties of the produced nano-carbon materials (rG1 and rGO2) against *S. aureus* and *E. coli*, representing Gram-positive and Gram-negative bacteria, respectively. Before every microbiological experiment, each sample and glassware was disinfected via autoclaving at 120 °C for 10 minutes. The bacteria were cultivated on a nutrient agar plate at 37 °C for 24 hours. Subsequently, the cultivated bacteria were introduced into 10 mL of saline solution to achieve a concentration of 10^8 colony-forming units per milliliter (CFU/mL). There was a dilution of the bacterial suspension to 106 CFU/mL. R1, R2, Neomycin, and Tetracycline stock solutions were made in dimethyl sulfoxide (DMSO) at concentrations of 50, 100, and 150 µg/mL. Inoculation of Muller Hinten agar plates was conducted with 106 CFU/ml of *E. coli* and *S. aureus*, respectively. Then, 6 mm diameter wells were created in the agar plates, and 100 µL of each concentration was added to separate wells. The plates were then incubated at 37 °C for 24 hours. Utilizing a Vernier caliper, the inhibition zones were measured. The antimicrobial efficacy was compared against standard antibiotics Neomycin and Tetracycline.

Statistical analysis

To evaluate the data, Graph Prism version 9.4.1 (681) was employed. To determine significant differences, Tukey's multiple comparisons post-doc test was used together with two-way analysis of variance (ANOVA). Mean ± standard deviation (SD) was used to indicate the means of the inhibition zone variations. The differences were considered significant, for the p-values were ≤0.05 or ≤0.0001.

Results and Discussion

Characterization of CMNC-rG1 and CMNCO-rGO2

In this fabrication, lamb meat was treated with hydrogen peroxide, then flame-charred and purified using solvents and acid wash.

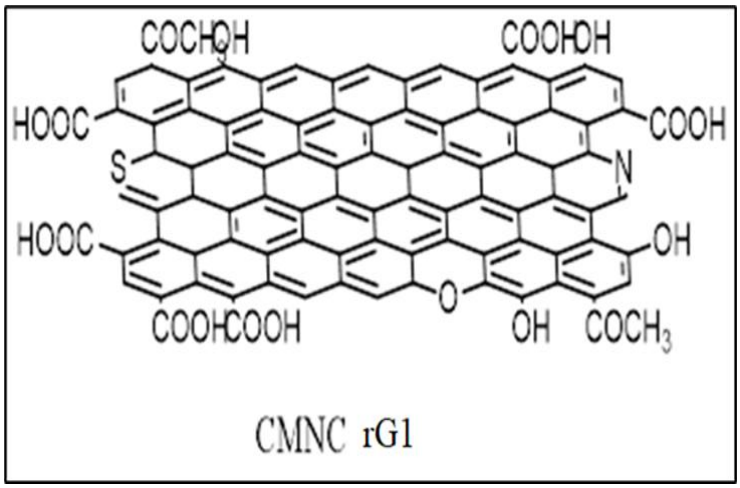

Figure 1. Chemical Structure of Synthesized Nano-Graphite (rG1)

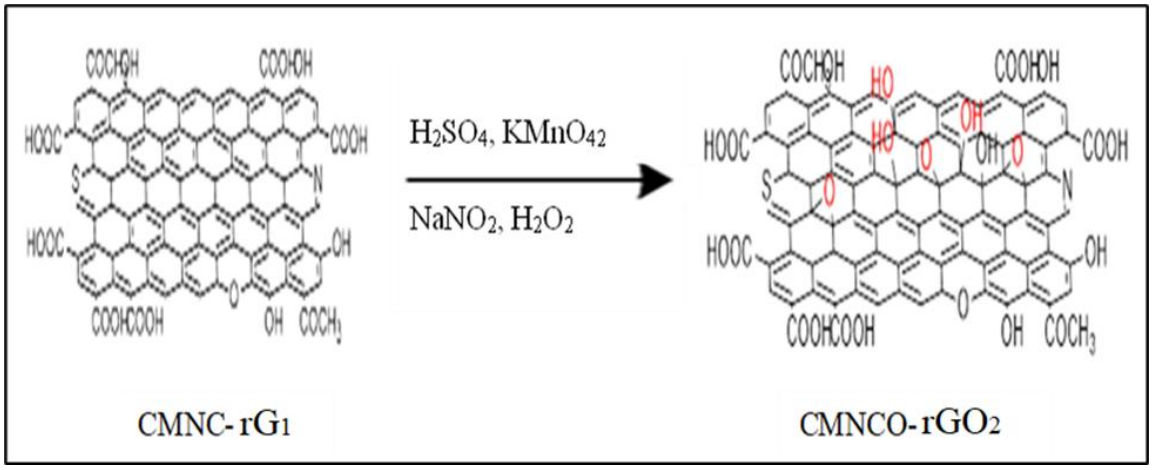

Figure 2. Exploring the Chemical Make-Up of nano-graphene oxide (rGO2)

The final product, CMNC-rG1, was obtained as a carbon-based nanocomposite.

Figure 1 displays a schematic diagram illustrating of the CMNC-rG1 nanocomposite. Nanoscale graphene oxide (rGO2) was synthesized from nanoscale graphite (rG1) using a modified Hummers method that includes oxidation, hydrolysis, and purification steps.

Figure 2 depicts a schematic diagram of the CMNCO-rGO2 nanocomposite using the chemical oxidation method.

Fourier transformation infrared spectroscopic (FTIR)

FTIR analysis was utilized to discover functional groups of CMNC-rG1 and CMNCO-rGO2 nanocomposite derived from lamb through chemical and thermal treatment. Figure 3 shows a broad and distinct band in the 3514-3458 cm^{-1} range, corresponding to the overlapping vibrations of hydroxyl (-OH) functional groups from alcohols and carboxylic acids. Additionally, a peak at 3068 cm^{-1} was observed. The spectrum also displayed an absorption band at 2929 cm^{-1}, associated with aromatic C-H stretching, while a characteristic C=C stretching band appeared in the 1641-1541 cm^{-1} region, confirming the presence of conjugated carbon frameworks.

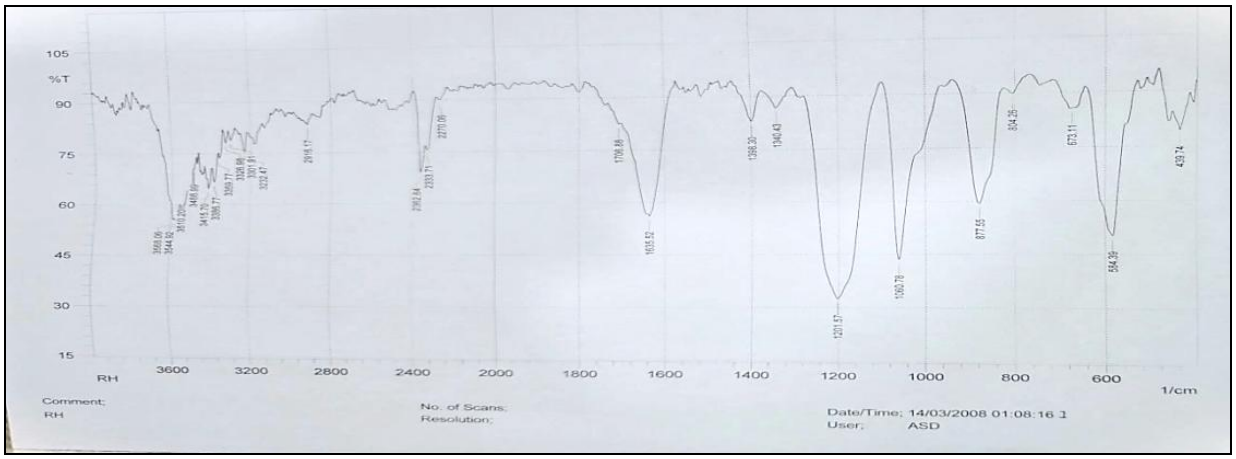

Figure 3. FT-IR Spectrum of nano-graphite (rG1)

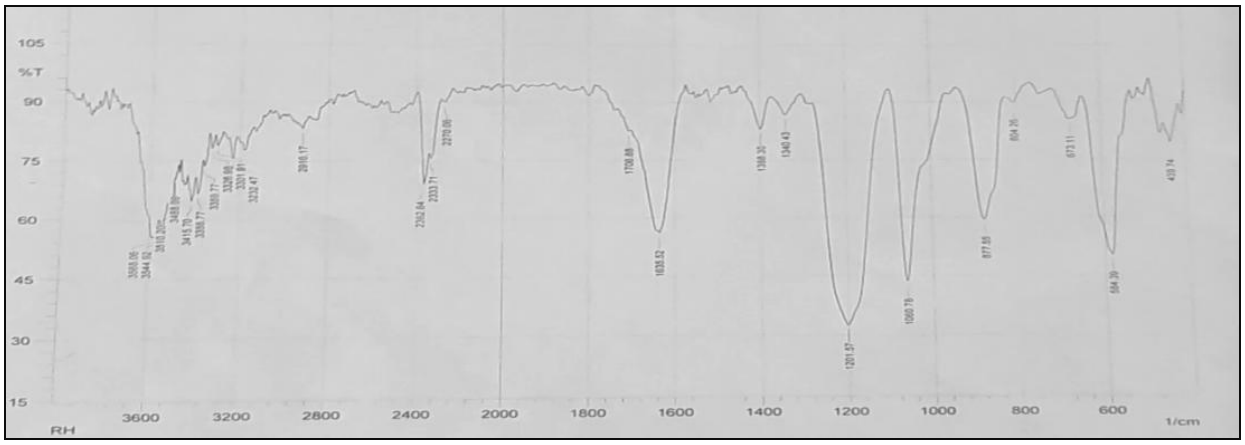

Figure 4. FT-IR spectrum of nano-graphene oxide (rGO2)

For nano-graphene oxide (rGO2), the FT-IR spectrum (Figure 4) exhibited a broad band at 3390 cm^{-1}, attributed to hydroxyl (-OH) stretching vibrations. Carbonyl (C=O) groups appeared at 1267 cm^{-1} and 1625 cm^{-1}, while aromatic C-H stretching was identified at 3051 cm^{-1}. The characteristic double bond (C=C) stretching bands were present at 1596 cm^{-1} and 1454 cm^{-1}, confirming the successful oxidation and functionalization of the material.

X-ray diffraction (XRD) analysis

The XRD spectrum values (d, D, and n)for Nano-Graphite (rG1) and Nano-Graphene Oxide (rGO2) were calculated by using Bragg's Law [19], Scherrer equation [20] and Insta NANO, n.d.).

Figure 5 exhibited a distinct diffraction peak at 2θ = 19.1712°, corresponding to an interlayer spacing (d) of 0.462 nm. The grain size (D) was calculated to be 17.43 nm. The estimated quantity of graphene layers (n) was 121.30, signifying a multi-layered configuration. These structural values are consistent with the typical properties reported for layered nanomaterials, indicating the successful formation of a well-ordered layered structure in compound rG1.

For Nano-Graphene Oxide (rGO2), the XRD pattern showed (Figure 6) a peak at 2θ = 55.1554°, with an interlayer spacing (d) of

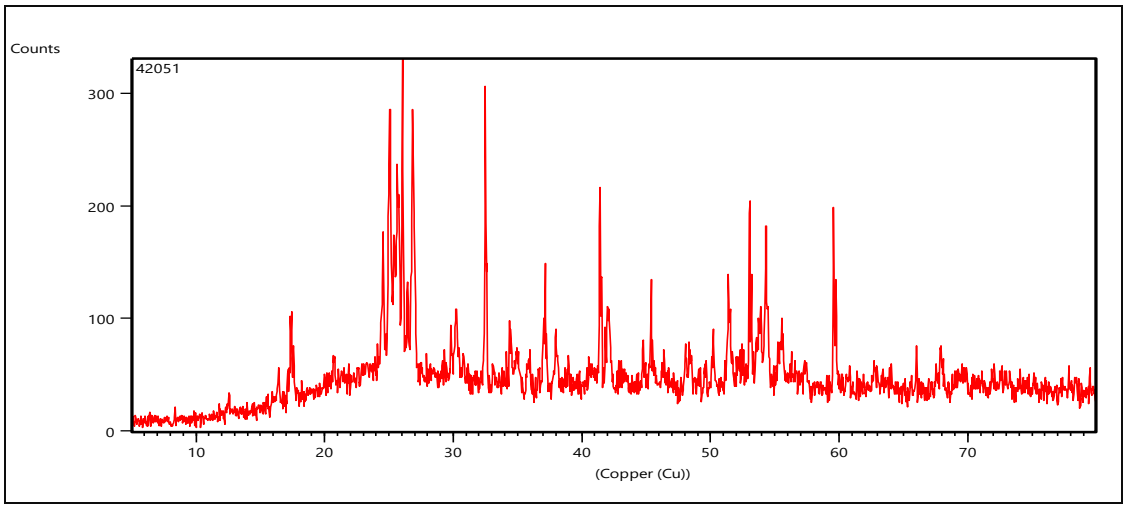

Figure 5. XRD Pattern of Nano-Graphite (rG1)

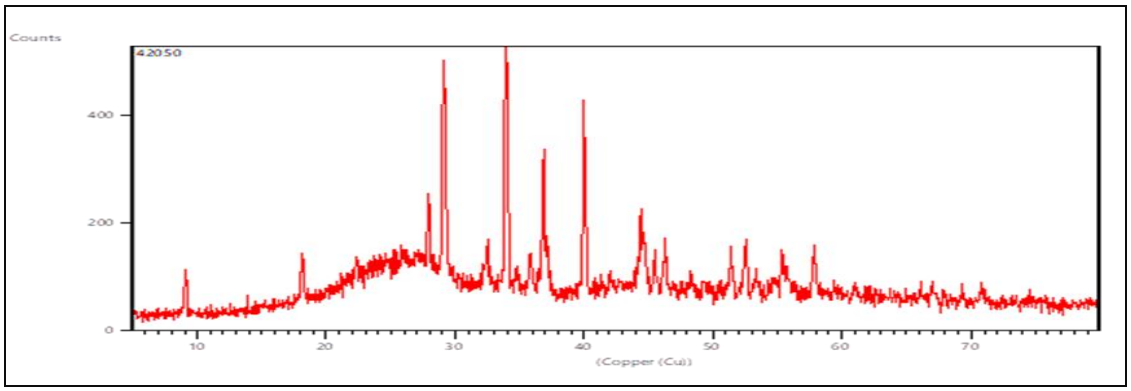

Figure 6. XRD pattern of nano-graphene oxide (rGO2)

2.58499 nm, grain size (D) of 94.46 nm, and a reduced layer count (n = 60.59). The shift in diffraction peaks confirmed the structural transformation from graphite to graphene oxide.

Field Emission Scanning Electron Microscopic (FESEM) Analysis FESEM images of Nano-Graphite (rG1) revealed a high degree of smoldering (Figure 7A), accompanied by visible cracks (Figure 7B) and minimal exfoliation (Figure 7C). The images also indicated coalescence of graphene layers (Figure 7D), contributing to the material's stability. However, localized decomposition led to the loss of certain volatile components, affecting surface roughness.

In contrast, nano-graphene oxide (rGO2) displayed less thickening and an increased exfoliation rate, estimated at 69%, compared to R1 (Figure 8A and B). The presence of clusters and edge folding suggested the oxidation-induced structural modifications (Figure 8C and D). The formation of graphene sheets with larger surface areas was evident, as observed in previous oxidation studies.

Atomic force microscopy (AFM) analysis

AFM images of nano-graphite (rG1) (Figure 9A-D) demonstrate sharp protrusions, indicating the presence of well-organized graphene layers. The surface distribution was semi-uniform, suggesting moderate exfoliation and structural integrity.

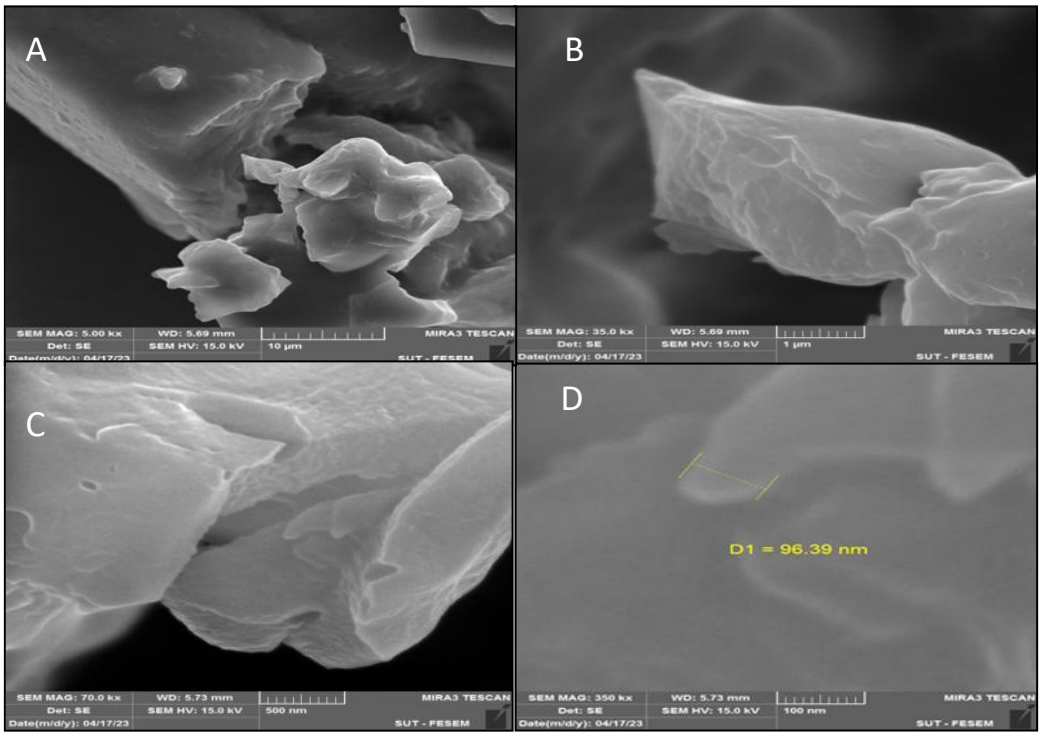

Figure 7. FESEM images of nano-graphite (rG1).

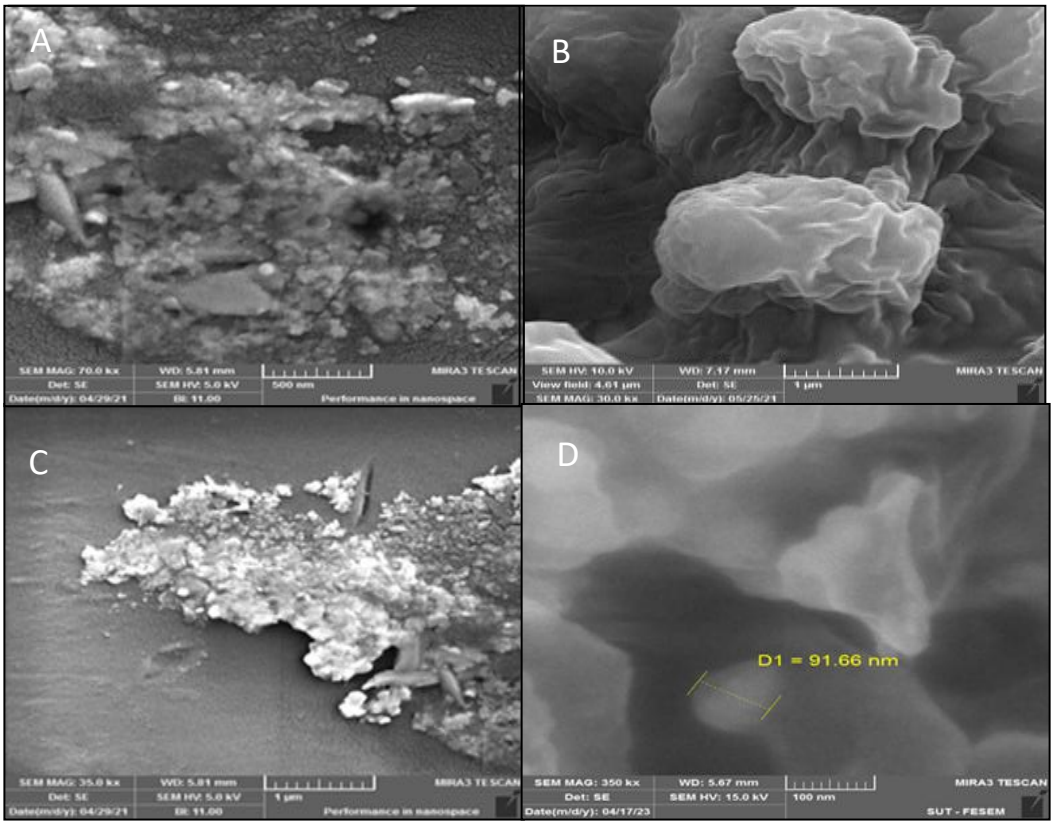

Figure 8. FESEM Images of nano-graphene oxide (rGO2).

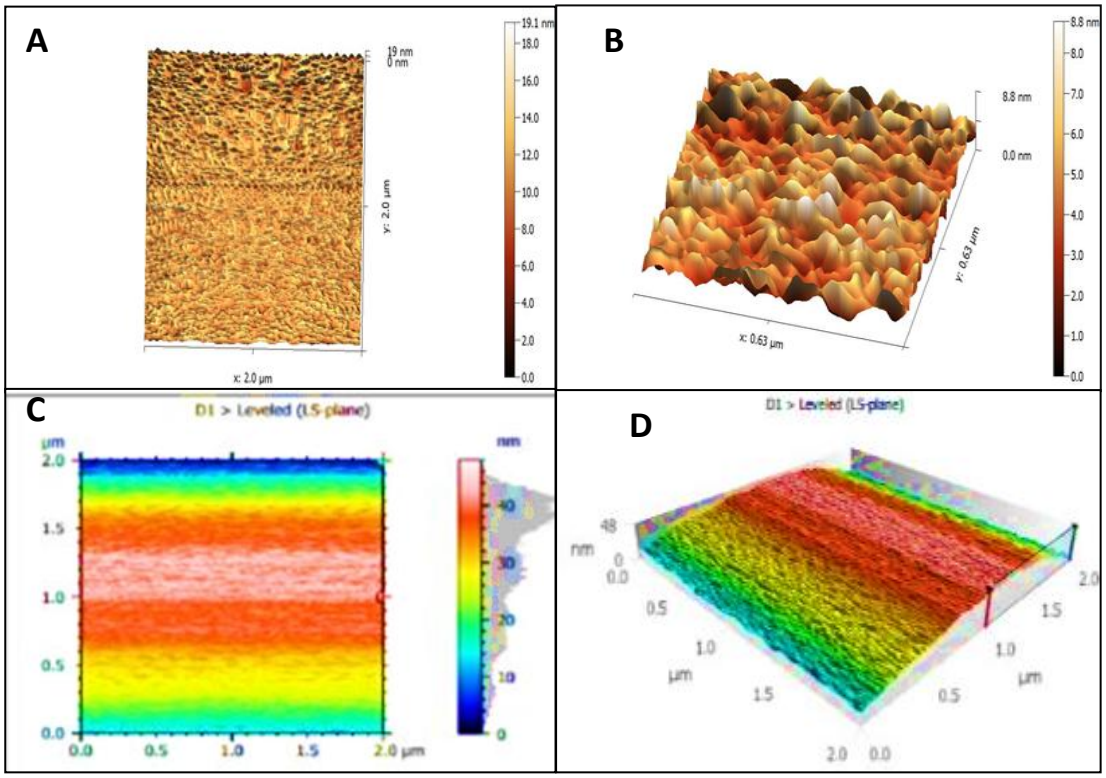

Figure 9. AFM Images of Nano-Graphite (rG1).

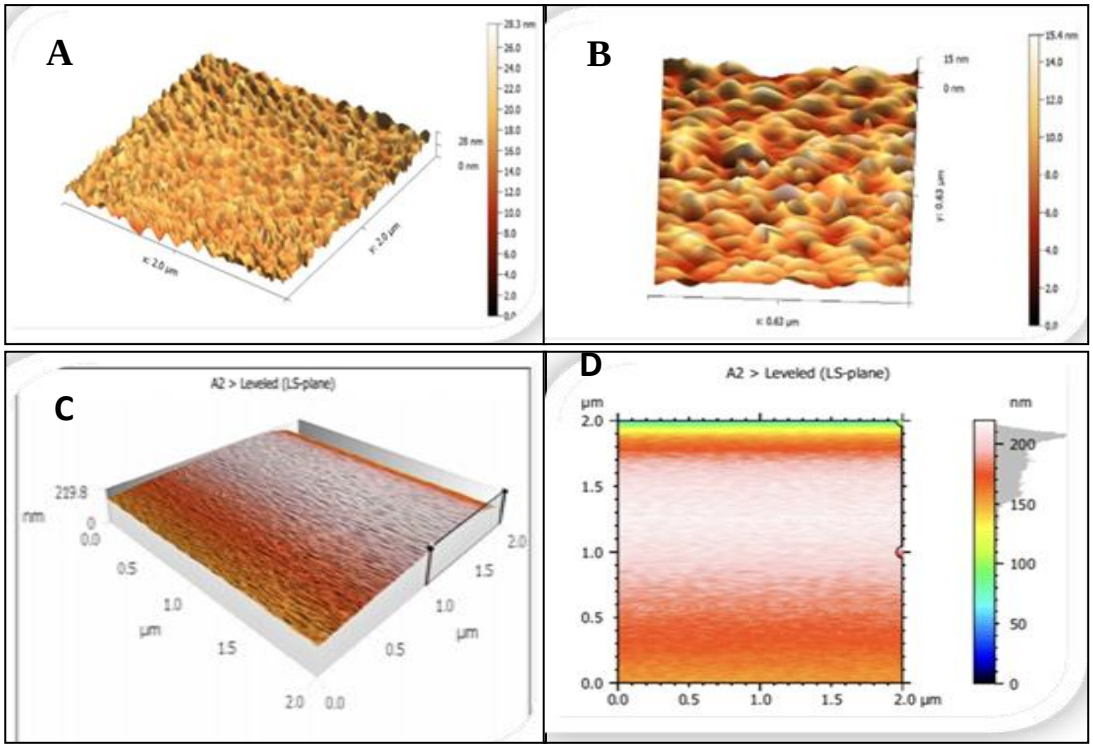

Figure 10. AFM Images of nano-graphene oxide (rGO2).

For nano-graphene oxide (rGO2) (Figure 10 A-D), AFM revealed an increase in peeling, forming larger graphene sheets. This suggests a reduction in particle size and layer count due to oxidation. The observed changes confirmed the effectiveness of the Modified Hummers Method in transforming rG1 into rGO2.

Thermal analysis (TG/DSC)

Thermal gravimetric analysis (TGA) of Nano-Graphite (rG1) (Figure 11) showed that 90.13% of the material decomposed at 1000 °C, confirming its thermal stability. The degradation occurred in two main stages: 0-400 °C–minor weight loss due to moisture evaporation and volatile organic decomposition and 400-700 °C–semi-solid phase transformation, where carbonization was predominant at 0.322 m. Differential scanning calorimetry (DSC) analysis revealed a heat-emitting reaction at 72.08 °C associated with the removal of water molecules. The second heat release, recorded at 12.12 °C, correlated with thermal transformation events, indicating the presence of non-oxidized fragments, and this was also reflected in the value 41.58 °C, while the endothermic reaction indicated poor stability and sensitivity of the material to heat [21].

Antibacterial evaluation of nano-graphite (rG1) and nano-graphene oxide (rGO2)

The antibacterial activity of nano-graphite (rG1) and nano-graphene oxide (rGO2) was absent against *E. coli*, while it was assessed by R2 against *Staphylococcus aureus* at concentrations of 50, 100, and 150 µ/mL. The inhibition zone measurements indicated that rGO2 demonstrated significant antibacterial effects, whereas R1 did not exhibit any inhibition (Table 1 and Figure 12).

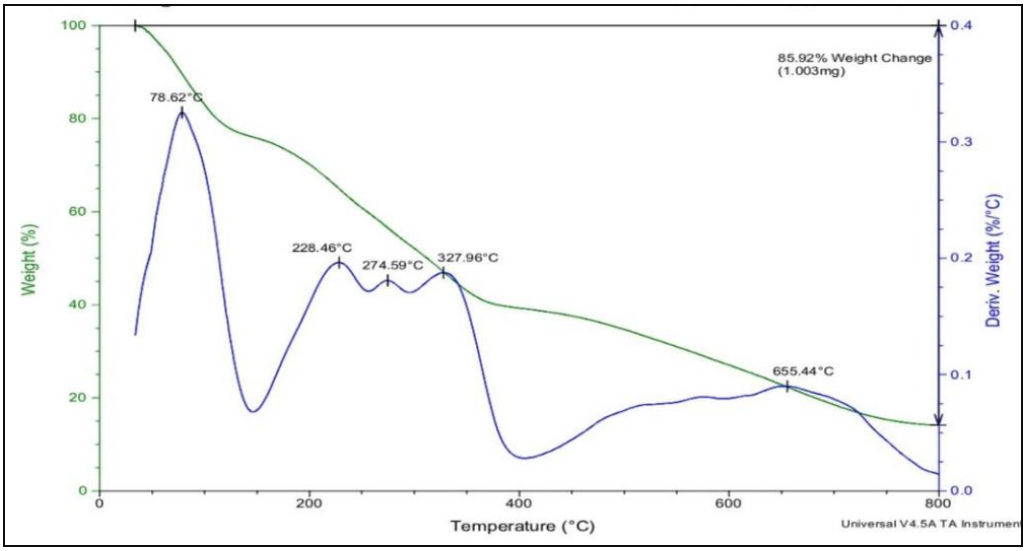

Figure 11. TG/DSC Analysis of Nano-Graphite (rG1). Enhanced Biological Activity Section with References.

Table 1. Antibacterial Activity for Nano-Graphene Oxide (R2). Against *S. aureus* (Inhibition Zone in mm)

Compound	50 µg/mL	100 µg/mL	150 µg/mL
rG1	-*	-	-
rGO2	10±0.5 mm	15.3 ± 1.04mm	17.4±1.2 mm
Tetracycline	-	24.7±1.2 mm	27.9 ±1.5 mm
Neomycin	17.4 ±1.15 mm	28±1.05 mm	30.2 ±0.6 mm

**absence of antibacterial activity.*

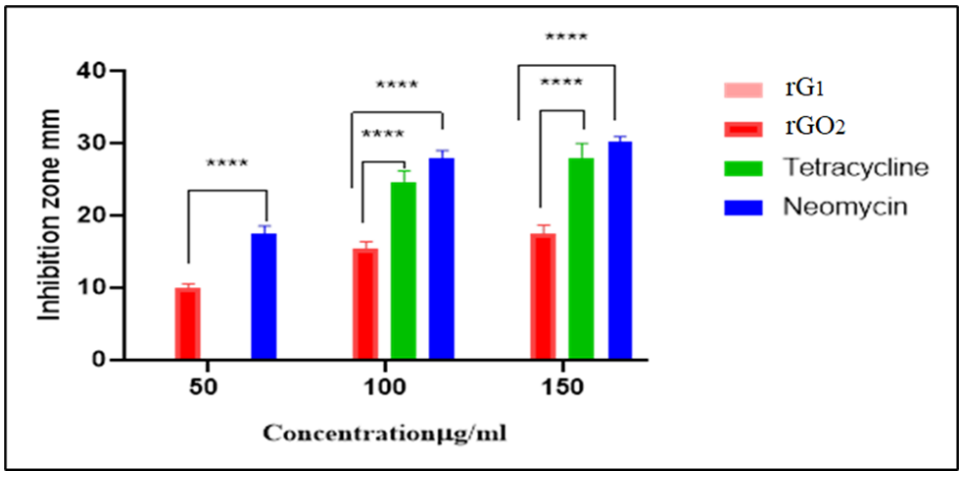

Figure 12. Inhibitory activity of the prepared compounds rG1and rGO2, Neomycin and tetracycline against *Staphylococcus aureus*.

There were significant differences ($p < 0.0001$) when comparing the mean values of inhibition by antibiotics used in this study (tetracycline and neomycin) and R2. For instance, at 50 μ/mL, the inhibition zone for R2 was (10±0.5) mm, increasing to 15.3 ± 1.04 mm at 100 μ/mL and reaching (17.4±1.2) mm at 150 μ/mL. In contrast, tetracycline (a commonly used antibiotic) showed large inhibition zones of 24.7±1.2 mm at 100 μ/mL and 27.9 ±1.5 mm at 150 μ/mL, while neomycin exhibited the highest inhibition of 30.2 ±0.6 mm at 150 μ/mL. These results suggest that R2 possesses moderate antibacterial properties, although it remains less potent than conventional antibiotics. The antibacterial properties of graphene-based nanomaterials have been reported in several studies, primarily due to their oxidative stress generation, membrane disruption, and bacterial entrapment. Researchers Akhavan and Ghaderi (2010) discovered that the antibacterial activity of graphene oxide was size-dependent. They showed that the better the inhibition of bacteria, the more surface interactions occurred with smaller sheet sizes [22].

Similar to how R2 inhibited *S. aureus* growth in their study, R2 was more harmful in this investigation. Nano-graphene oxide's (rGO2) antimicrobial properties stem from the following pathways: Generation of Reactive Oxygen Species (ROS) and Oxidative Stress. Nano-graphene oxide (rGO2) possesses oxygen-rich functional groups that can generate reactive oxygen species (ROS), which can harm bacterial proteins and membranes [23].

Lipid peroxidation, caused by reactive oxygen species (ROS), breaks down the bacterial cell wall and allows cytoplasmic leakage. Breakdown of bacterial membranes via physical means. When rGO2 nanosheets pierce bacterial membranes, they cause structural damage and intracellular content leakage due to their sharp edges [24].

Past research using field-effect scanning electron microscopy (FESEM) has confirmed this effect by showing membrane shrinkage and cytoplasmic leakage in bacterial colonies treated with graphene-based materials. Absorption of bacteria onto surfaces of graphene oxide-based nanomaterials can inhibit nutrient intake and starve the germs to death [25]. However, in this study, Nano-graphene oxide (rGO2) did not show antibacterial activity against *E. coli*. As recorded, gram-negative bacteria such as *E. coli* are more resistant to physical damage from sharp nanoscale surfaces due to their protective outer membrane, while Gram-positive bacteria such as S. aureus, which lack this membrane, are more susceptible to membrane disruption [22].

Conclusion

The physical measurements confirmed the validity of the structures of the prepared nanocomposites. The preparation method was of moderate complexity and resulted in a high yield of nano-products. Possible applications of rGO2 in healthcare and manufacturing sectors include biomedical and environmental uses, such as wound dressings and medical device coatings, due to its moderate antibacterial activity.

Acknowledgments

For the use of their FT-IR facilities, the authors would like to thank the Department of Chemistry at Tikrit University in Iraq. Further thanks are due to the researchers at Iran's Kashan University, who ran the FESEM, AFM, and XRD analyses. The author would like to extend their gratitude to the University of Tikrit, Iraq, specifically to the Department of Biology under the College of Education for Pure Science, for providing the bacterial isolates utilized in this investigation.

Authors' Contributions

Reem Suhail. Najm: Visualization, methodology, and practical work investigation. Agharid A.AL-Rasheed, Writing- review–& editing as well as microbiology practical work. Ammar S.Mohammed: Practical work corporation. Bashiru Graba:Visualization: Writing- review–& editing and microbiology practical work. Mohammed Jwher Saleh: Practical work corporation.

Orcid

Reem Suhail Najm: 0000-0003-2059-3395
Agharid. A. AL-Rasheed: 0000-0001-6551-1045
Ammar S. Mohammed: 0000-0003-4011-4187
Bashiru Graba: 0000-0001-7295-9665
Mohammed Jwher Saleh: 0009-0005-5247-9310

References

[1] P.T. Anastas, J.C. Warner, Principles of green chemistry, *Green Chemistry: Theory and Practice*, **1998**, *29*, 14821-14842. [Crossref], [Google Scholar], [Publisher]

[2] R. Mishra, B. Pramanick, T.K. Maiti, T.K. Bhattacharyya, Glassy carbon microneedles—new transdermal drug delivery device derived from a scalable C-MEMS process, *Microsystems & Nanoengineering*, **2018**, *4*, 38. [Crossref], [Google Scholar], [Publisher]

[3] K.M. Abou El-Nour, A.a. Eftaiha, A. Al-Warthan, R.A. Ammar, Synthesis and applications of silver nanoparticles, *Arabian Journal of Chemistry*, **2010**, *3*, 135-140. [Crossref], [Google Scholar], [Publisher]

[4] G.C.A. Collaborative, Global climate alliance for accelerated climate action, New Delhi: Observer Research Foundation, Brussels: Konrad-Adenauer Stiftung, **2022**. [Google Scholar]

[5] L. Mathur, S.S. Hossain, M.R. Majhi, P.K. Roy, Synthesis of nano-crystalline forsterite (Mg_2SiO_4) powder from biomass rice husk silica by solid-state route, *Boletín De La Sociedad Española De Cerámica Y Vidrio*, **2018**, *57*, 112-118. [Crossref], [Google Scholar], [Publisher]

[6] S. Niksa, Predicting the macroscopic combustion characteristics of diverse forms of biomass in pp firing, *Fuel*, **2021**, *283*, 118911. [Crossref], [Google Scholar], [Publisher]

[7] M.A. Nazem, M.H. Zare, S. Shirazian, Preparation and optimization of activated nano-carbon production using physical activation by water steam from agricultural wastes, *RSC Advances*, **2020**, *10*, 1463-1475. [Crossref], [Google Scholar], [Publisher]

[8] R. Wang, D. Chen, Q. Wang, Y. Ying, W. Gao, L. Xie, Recent advances in applications of carbon

nanotubes for desalination: A review, *Nanomaterials*, **2020**, *10*, 1203. [Crossref], [Google Scholar], [Publisher]

[9] K.-H. Cho, J.-E. Park, T. Osaka, S.-G. Park, The study of antimicrobial activity and preservative effects of nanosilver ingredient, *Electrochimica Acta*, **2005**, *51*, 956-960. [Crossref], [Google Scholar], [Publisher]

[10] a) X. Pan, J. Ji, N. Zhang, M. Xing, Research progress of graphene-based nanomaterials for the environmental remediation, *Chinese Chemical Letters*, **2020**, *31*, 1462-1473. [Crossref], [Google Scholar], [Publisher] b) Mollalar M.N., Banaei A., Massoudi A. Synthesis, characterization, and adsorption studies of functionalized graphene oxide via covalent interactions, *Chemical Methodologies*, **2025**, *9*, 771-789. [Crossref], [Publisher]

[11] J. Simon, E. Flahaut, M. Golzio, Overview of carbon nanotubes for biomedical applications, *Materials*, **2019**, *12*, 624. [Crossref], [Google Scholar], [Publisher]

[12] L. Dybowska-Sarapuk, W. Sosnowicz, J. Krzeminski, A. Grzeczkowicz, L.H. Granicka, A. Kotela, M. Jakubowska, Printed graphene layer as a base for cell electrostimulation—preliminary results, *International Journal of Molecular Sciences*, **2020**, *21*, 7865. [Crossref], [Google Scholar], [Publisher]

[13] Z. Peng, X. Liu, W. Zhang, Z. Zeng, Z. Liu, C. Zhang, Y. Liu, B. Shao, Q. Liang, W. Tang, Advances in the application, toxicity and degradation of carbon nanomaterials in environment: A review, *Environment International*, **2020**, *134*, 105298. [Crossref], [Google Scholar], [Publisher]

[14] S.K. Alen, S. Nam, S.A. Dastgheib, Recent advances in graphene oxide membranes for gas separation applications, *International Journal of Molecular Sciences*, **2019**, *20*, 5609. [Crossref], [Google Scholar], [Publisher]

[15] M.M. Rahman, M.G. Ara, M.A. Alim, M.S. Uddin, A. Najda, G.M. Albadrani, A.A. Sayed, S.A. Mousa, M.M. Abdel-Daim, Mesoporous carbon: A versatile material for scientific applications, *International Journal of Molecular Sciences*, **2021**, *22*, 4498. [Crossref], [Google Scholar], [Publisher]

[16] a) X. Yang, G. Zhang, J. Prakash, Z. Chen, M. Gauthier, S. Sun, Chemical vapour deposition of graphene: Layer control, the transfer process, characterisation, and related applications, *International Reviews in Physical Chemistry*, **2019**, *38*, 149-199. [Crossref], [Google Scholar], [Publisher] b) Iqbal S.Z., Qadir K.W., Abdullah H.Y., Dastgheib A.M., Bashir, M.M. Characterization of solar absorber coated by reduced graphene oxide polymer composite on metal sheets. International *Journal of Thermophysics*, **2021**, *42*, 33. [Crossref], [Google Scholar], [Publisher]

[17] Y. Li, K.C. Mei, R. Liam-Or, J.T.W. Wang, F.N. Faruqu, S. Zhu, Y.-l. Wang, Y. Lu, K.T. Al-Jamal, Graphene oxide nanosheets toxicity in mice is dependent on protein corona composition and host immunity, *ACS Nano*, **2024**, *18*, 22572-22585. [Crossref], [Google Scholar], [Publisher]

[18] a) L. Shahriary, A.A. Athawale, Graphene oxide synthesized by using modified hummers approach, *International Journal of Renewable Energy and Environment Engineering*, **2014**, *2*, 58-63. [Google Scholar], [Publisher] b) Jahani P.M., Zaimbashi R., Tajik S., Beitollai H. Electrochemical sensor for determination of paracetamol based on reduced graphene oxide/polypyrrole nanotubes nanocomposite modified screen printed electrode in pharmaceutical samples, *Chemical Methodologies*, **2025**, *9*, 251-267. [Crossref], [Publisher]

[19] a) B.D. Cullity, R. Smoluchowski, Elements of X-ray Diffraction, *Physics Today*, **1957**, *10*, 50-50. [Crossref], [Google Scholar], [Publisher] b) Zbuzant M. Production methods of carbon nano-tubes in industry, *Journal of Engineering*

in Industrial Research, **2024**, 5, 237-245. [Crossref], [Publisher]

[20] H.P. Klug, L.E. Alexander, X-ray diffraction procedures: For polycrystalline and amorphous materials, **1974**. [Google Scholar], [Publisher]

[21] A. Alemdar, M. Sain, Isolation and characterization of nanofibers from agricultural residues–Wheat straw and soy hulls, *Bioresource Technology*, **2008**, *99*, 1664-1671. [Crossref], [Google Scholar], [Publisher]

[22] O. Akhavan, E. Ghaderi, Toxicity of graphene and graphene oxide nanowalls against bacteria, *ACS Nano*, **2010**, *4*, 5731-5736. [Crossref], [Google Scholar], [Publisher]

[23] W. Hu, C. Peng, W. Luo, M. Lv, X. Li, D. Li, Q. Huang, C. Fan, Graphene-based antibacterial paper, *ACS Nano*, **2010**, *4*, 4317-4323. [Crossref], [Google Scholar], [Publisher]

[24] S. Gurunathan, J.W. Han, A.A. Dayem, V. Eppakayala, J.-H. Kim, Oxidative stress-mediated antibacterial activity of graphene oxide and reduced graphene oxide in Pseudomonas aeruginosa, *International Journal of Nanomedicine*, **2012**, 5901-5914. [Crossref], [Google Scholar], [Publisher]

[25] D.A. Dikin, S. Stankovich, E.J. Zimney, R.D. Piner, G.H. Dommett, G. Evmenenko, S.T. Nguyen, R.S. Ruoff, Preparation and characterization of graphene oxide paper, *Nature*, **2007**, *448*, 457-460. [Crossref], [Google Scholar], [Publisher]

HOW TO CITE THIS ARTICLE

R.S. Najm, A.A. AL-Rasheed, A.S. Mohammed, B. Garba, M.J. Saleh. Synthesis, Chemical Characterization and Biological Activity Evaluation of Lamb Meat-Derived Nanocomposite. *Adv. J. Chem. A*, 2025, 8(12), 1890-1903.

DOI: 10.48309/AJCA.2025.524268.1849
URL: https://www.ajchem-a.com/article_224877.html